

Self-Calibrated Cluster Counts as a Probe of Primordial Non-Gaussianity

Masamune Oguri*

*Kavli Institute for Particle Astrophysics and Cosmology, Stanford University,
2575 Sand Hill Rd. M/S 29, Menlo Park, CA 94025.*

(Dated: November 1, 2018)

We show that the ability to probe primordial non-Gaussianity with cluster counts is drastically improved by adding the excess variance of counts which contains information on the clustering. The conflicting dependences of changing the mass threshold and including primordial non-Gaussianity on the mass function and biasing indicate that the self-calibrated cluster counts well break the degeneracy between primordial non-Gaussianity and the observable-mass relation. Based on the Fisher matrix analysis, we show that the count variance improves constraints on f_{NL} by more than an order of magnitude. It exhibits little degeneracy with dark energy equation of state. We forecast that upcoming Hyper Suprime-cam cluster surveys and Dark Energy Survey will constrain primordial non-Gaussianity at the level $\sigma(f_{\text{NL}}) \sim 8$, which is competitive with forecasted constraints from next-generation cosmic microwave background experiments.

PACS numbers: 95.36.+x, 98.65.Cw, 98.80.-k

The measurement of departures from Gaussianity of the initial perturbations provides a unique opportunity to probe the early universe [1]. While the standard single field slow-roll inflation models predict primordial perturbations very close to Gaussian, some models such as multi-field models and the curvaton model can produce the level of non-Gaussianity high enough to be detected in ongoing or future surveys. Thus specific forms of primordial non-Gaussianity contain valuable information on how the initial density fluctuations are generated.

Observationally, primordial non-Gaussianity has mainly been studied using the temperature fluctuation of the Cosmic Microwave Background (CMB). Recently it has attracted considerable attention given a possible detection of non-Gaussianity by Yadav and Wandelt [2]. However, the detection of non-Gaussianity in the CMB is somewhat controversial in the sense that independent analyses yield slightly different results [3], suggesting the importance of other observational probes independent of the CMB. Another powerful probe of primordial non-Gaussianity is provided by the large-scale structure of the universe. In particular, non-Gaussianity induces a scale-dependent halo bias [4, 5, 6, 7, 8], and thus by studying large-scale distributions of astronomical objects one can obtain tight constraints that are competitive with the CMB. Constraints from the large-scale structure are also important given that non-Gaussianity can be scale-dependent such that deviations from Gaussian are larger at smaller scales [9].

Primordial non-Gaussianity is also sensitive to the abundance of massive clusters and its redshift evolution [4, 10]. An advantage of using massive clusters is its reasonable one-to-one correspondence with dark halos, which suggests that halo assembly bias (e.g., [6]) is less important. A challenge here is how to calibrate cluster masses; since the cluster mass is not directly observable, one has to resort to well-calibrated correlations between cluster masses and observable quantities such as

luminosities, temperatures, and the numbers of member galaxies in order to infer cluster masses. The observable-mass relations always involve uncertainties, suggesting that the change of cluster abundances by primordial non-Gaussianity may be compensated by modifying the relation between observables and masses. Therefore constraints from cluster counts rely on how well we can calibrate such observable-mass relations.

In this *Letter*, we point out that clustering information breaks the degeneracy and allows us to determine primordial non-Gaussianity surprisingly well with cluster counts. This is because the clustering bias for massive clusters is quite sensitive to both cluster masses and primordial non-Gaussianity, and more importantly, because the cluster abundance and biasing show conflicting dependences on these. Such self-calibrated cluster count technique has been discussed extensively in the context of accurate dark energy probes [11, 12, 13, 14], but its use for primordial non-Gaussianity has not been explored.

Here we quantify non-Gaussianity of the local form using the standard parametrization, $\Phi = \phi + f_{\text{NL}}(\phi^2 - \langle \phi^2 \rangle)$, where Φ is the curvature perturbation and ϕ is an auxiliary random-Gaussian field. The parameter $f_{\text{NL}} > 0$ (< 0) indicates that the initial density field is positively (negatively) skewed. The current level of constraints on primordial non-Gaussianity is $|f_{\text{NL}}| \lesssim \mathcal{O}(100)$ [2, 3, 6]. We adopt a non-Gaussian correction factor of the cluster mass function based on the Edgeworth expansion [9]:

$$\frac{dn/dM}{dn_G/dM} = 1 + \frac{\sigma S_3}{6}(\nu^3 - 3\nu) - \frac{1}{6} \frac{d(\sigma S_3)}{d \ln \nu} \left(\nu - \frac{1}{\nu} \right), \quad (1)$$

where $\nu = \delta_c/\sigma$, $\delta_c \approx 1.68$ is the critical linear overdensity, $\sigma = \sigma(M, z)$ is the linear fluctuation on the mass scale of M which we compute using the transfer function $T(k)$ presented by Eisenstein and Hu [15] ignoring the baryon wiggle. We adopt models of Warren *et al.* [16]

for the mass function in the Gaussian case, dn_G/dM . The skewness S_3 is related to f_{NL} as [8]

$$\begin{aligned} \sigma S_3 &= \frac{f_{\text{NL}}}{\sigma^3} \int_0^\infty \frac{dk_1}{k_1} \alpha(k_1) W(M, k_1) \Delta_\phi^2(k_1) \\ &\times \int_0^\infty \frac{dk_2}{k_2} \alpha(k_2) W(M, k_2) \Delta_\phi^2(k_2) \\ &\times \int_{-1}^1 d\mu \alpha(k) W(M, k) \left[1 + \frac{P_\phi(k)}{P_\phi(k_1)} + \frac{P_\phi(k)}{P_\phi(k_2)} \right] (2) \end{aligned}$$

where $\Delta_\phi^2 = k^3 P_\phi(k)/2\pi^2$ is the power spectrum of the curvature perturbation, $\alpha = [2D(z)T(k)/3\Omega_M](ck/H_0)^2$, $D(z)$ is the linear growth rate normalized to $(1+z)^{-1}$ in the matter-dominant era, and $k^2 = k_1^2 + k_2^2 + 2\mu k_1 k_2$. For the window function $W(M, k)$ we adopt the real space top-hat filter. In practice we use the following fitting formula for σS_3 :

$$\begin{aligned} \sigma S_3 &\approx (8.66 \times 10^{-5}) f_{\text{NL}} \frac{\Omega_M}{D(0)} \Gamma^{-1.4} \sigma_8 \\ &\times m_{10}^{-0.0272 - 0.11(n_s - 0.96) - 0.0008 \log m_{10}}, \quad (3) \end{aligned}$$

with $m_{10} = [M/(10^{10} h^{-1} M_\odot)] \Gamma^3 (\Omega_M h^2)^{-1}$ and $\Gamma = \Omega_M h \exp[-\Omega_b(1 + \sqrt{2h}/\Omega_M)]$ is so-called the shape parameter [17]. This fitting formula should be accurate at a few percent level in the mass scale range $10^7 h^{-1} M_\odot \lesssim M \lesssim 10^{18} h^{-1} M_\odot$.

The non-Gaussian correction of the halo bias is computed as [8]

$$\Delta b(M, z, k) = \frac{2f_{\text{NL}}\delta_c}{\alpha} (b_G - 1) - \frac{\nu}{\delta_c} \frac{d}{d\nu} \left(\frac{dn/dM}{dn_G/dM} \right), \quad (4)$$

The halo bias in the Gaussian case, b_G , is assumed to be the form presented by Sheth and Tormen [18].

Fig. 1 illustrates the reason why the clustering information is so important. As shown in the Figure, including positive f_{NL} increases the number of clusters above some mass threshold M_{th} . This increment can be compensated by raising M_{th} . However, these two models with the same numbers of clusters result in quite different halo biases because *both* raising M_{th} and f_{NL} increase the biasing. Thus by including clustering information we can strongly break the degeneracy between M_{th} and f_{NL} , and can obtain tight constraints on f_{NL} .

We now forecast constraints on f_{NL} from future cluster surveys. We include the clustering information using a count-in-cell analysis. Specifically we approximate the Fisher matrix as [12, 13]

$$F_{\alpha\beta} = \mathbf{m}_{,\alpha}^T \mathbf{C}^{-1} \mathbf{m}_{,\beta} + \frac{1}{2} \text{Tr} [\mathbf{C}^{-1} \mathbf{S}_{,\alpha} \mathbf{C}^{-1} \mathbf{S}_{,\beta}] + \frac{\delta_{\alpha\beta}}{\sigma_p^2(\alpha)}, \quad (5)$$

where σ_p represents the prior information on each parameter, and the covariance matrix is given by $\mathbf{C} \equiv$

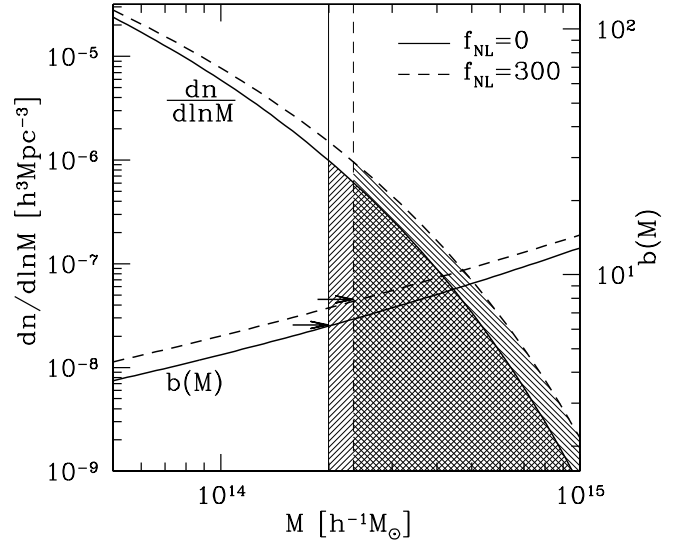


FIG. 1: The illustration of self-calibrating cluster counts to probe primordial non-Gaussianity f_{NL} . Here the redshift is $z = 1$. In cluster surveys, we basically obtain the number of clusters above some mass threshold M_{th} . The plot indicates that the increase of the mass function dn/dM due to positive f_{NL} can be compensated by increasing the M_{th} . However, while the two models predict the same number of clusters, the corresponding halo bias $b(M)$ (here we adopted $k = 0.02h\text{Mpc}^{-1}$) are quite different because both raising M_{th} and f_{NL} increase $b(M)$ (see arrows). Although in this plot the scatter in the observable-mass relation is ignored for simplicity, it will be included in the Fisher matrix analysis.

$\mathbf{S} + \text{diag}(\mathbf{m})$. The number count \mathbf{m} and its variance \mathbf{S} are computed as

$$m_i = V_i \int_i \frac{dM_{\text{obs}}}{M_{\text{obs}}} \int dM \frac{dn}{dM} p(M_{\text{obs}}|M), \quad (6)$$

$$S_{ij} = \frac{1}{V_i V_j} \int \frac{d^3k}{(2\pi)^3} W_i^*(\mathbf{k}) W_j(\mathbf{k}) P(k) b_i b_j, \quad (7)$$

$$b_i = V_i \int_i \frac{dM_{\text{obs}}}{M_{\text{obs}}} \int dM \frac{dn}{dM} b(M, k) p(M_{\text{obs}}|M), \quad (8)$$

where the subscript i run over redshift, mass, and angular bins. The power spectrum is described by $P(k)$, and the k -space window function by $W_i(\mathbf{k})$. Since the off-diagonal elements of \mathbf{S} are small in our case, here we consider only the diagonal elements. The function $p(M_{\text{obs}}|M)$ models the accuracy of the cluster mass determination from observables. Following [13], we assume the log-normal distribution for $p(M_{\text{obs}}|M)$, with the median of $\ln M + \ln M_{\text{bias}}$ and the scatter of $\sigma_{\ln M}$, and regard $\sigma_{\ln M}$ and $\ln M_{\text{bias}}$ (which corresponds to M_{th} in Fig. 1) as nuisance parameters. Note that the first term of the Fisher matrix (Eqn. 5) represents the information from number counts, whereas the second term the

information from the variance of the counts which contain clustering (biasing) information. Using the Fisher matrix, one can estimate a marginalized error on each parameter as $\sigma(\alpha) = \sqrt{(\mathbf{F}^{-1})_{\alpha\alpha}}$.

We calculate the Fisher matrix in 10-dimensional parameter space; 6 standard cosmological parameters including dark energy equation of state (the matter density $\Omega_M h^2$, the baryon density $\Omega_b h^2$, the power spectrum tilt n_s , the normalization of the power spectrum δ_ζ [19], the dark energy density Ω_{DE} , and dark energy equation of state w), 1 parameter representing primordial non-Gaussianity (f_{NL}), and 3 parameters from the observable-mass relation, $\sigma_{\ln M}$ and $\ln M_{\text{bias}} = \ln M_{\text{bias},0} + \gamma \ln(1+z)$. The Five-Year Wilkinson Microwave Anisotropy Probe (WMAP5) result for ΛCDM [20], $(\Omega_M h^2, \Omega_b h^2, n_s, \delta_\zeta, \Omega_{\text{DE}}, w) = (0.133, 0.0227, 0.963, 4.61 \times 10^{-5}, 0.742, -1)$, is adopted as our fiducial cosmological model. We add conservative priors to the first 4 parameters, $\sigma_p(\Omega_M h^2) = 0.006$, $\sigma_p(\Omega_b h^2) = 0.0006$, $\sigma_p(n_s) = 0.015$, and $\sigma_p(\delta_\zeta) = 10^{-6}$; these are the level of accuracies which has already been achieved by WMAP5. In addition, our fiducial model has $f_{\text{NL}} = 0$, $\sigma_{\ln M} = 0.25$, $\ln M_{\text{bias},0} = 0$, and $\gamma = 0$.

For illustrative purposes, we consider the following three upcoming surveys; Hyper Suprime-Cam on Subaru telescope (HSC; since the design of the HSC cluster survey is still tentative, we consider both 1000 deg^2 and 2000 deg^2), Dark Energy Survey (DES; 5000 deg^2) [21], and Large Synoptic Survey Telescope (LSST; 20000 deg^2) [22]. We adopt a simplified assumption that these optical surveys will find clusters with $M_{\text{obs}} > 10^{13.7} h^{-1} M_\odot$ out to $z_{\text{max}} = 1.4, 1.0,$ and 1.7 , respectively. For the count-in-cell analysis, we use the cell size of 20 deg^2 and the redshift interval $\Delta z = 0.1$. Three mass bins with spacing of $\Delta \log M_{\text{obs}} = 0.5$ are also adopted.

In Fig. 2, we show marginalized constraints on f_{NL} and the correlations with the parameters $\sigma_{\ln M}$, expected for the 2000 deg^2 HSC cluster survey. As expected, constraints are drastically improved by combining the number counts with the variance which includes the clustering information. This is partly because constraints from number counts and variance show different degeneracy directions, suggesting that *both* the number counts and clustering are essential for accurate determinations of f_{NL} .

Table I summarizes forecasted constraints on various cosmological parameters. For all the upcoming surveys, the count variance drastically enhances the ability to probe primordial non-Gaussianity, by more than an order of magnitude improvement in f_{NL} compared with the number counts alone. Predicted marginalized errors of $\sigma(f_{\text{NL}}) \sim 8$ for HSC and DES and ~ 2 for LSST are competitive with constraints from next-generation CMB experiments (e.g., [23]) and galaxy power spectrum measurements (e.g., [4, 24]). The variance helps to regulate the observable-mass relation, improving an accuracy of

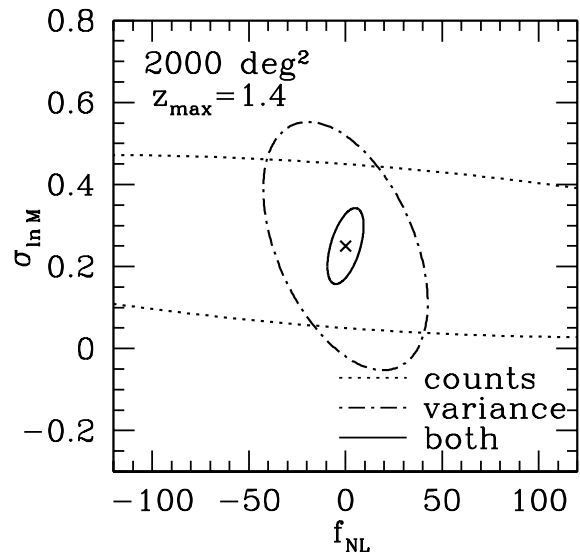


FIG. 2: Expected marginalized constraints in the $f_{\text{NL}}\text{-}\sigma_{\ln M}$ plane from the upcoming 2000 deg^2 HSC cluster survey. WMAP5 cosmology is assumed as a fiducial model. Contours indicate the 68% confidence regions from the number counts (*dotted*), the variance of the counts which contains the clustering information (*dash-dotted*), and the combination of the number counts and variance (*solid*).

$\ln M_{\text{bias},0}$ and $\sigma_{\ln M}$ measurements by a factor of two or more. Measurements of dark energy equation of state are improved as well, which is consistent with earlier work. We find that w and f_{NL} are not correlated very much, indicating that we can well determine these two parameters simultaneously using self-calibrated cluster counts. Fig. 3 shows contours of $\sigma(f_{\text{NL}})$ as a function of the survey area and the maximum redshift. The expected constraints on f_{NL} is a steep function of the maximum redshift even at $z > 1$, which indicate the importance of the deep surveys to detect clusters out to $z \gtrsim 1$.

We have shown that adding clustering information from the count variance drastically improves measurements of primordial non-Gaussianity with cluster counts. Although the calibration of cluster masses limits the use of cluster counts as a cosmological probe, the self-calibration technique allows us to determine both the observable-mass relation and f_{NL} simultaneously. The significant effect of the count variance comes from the conflicting dependences of the mass threshold and f_{NL} on the cluster mass function and biasing parameter (Fig. 1). Allowing dark energy equation of state to vary does not degrade f_{NL} measurements very much. Resulting forecasted constraints on f_{NL} , $\sigma(f_{\text{NL}}) \sim 8$ for HSC and DES and ~ 2 for LSST, suggest that cluster counts can become a competitive probe compared to the CMB or the large-scale galaxy power spectrum.

We have here made a number of simplified assumptions. For instance, it is important to check how the possible redshift evolution of the observable-mass relation

Survey	Counts			Variance			Counts + Variance		
	$\sigma(\Omega_{\text{DE}})$	$\sigma(w)$	$\sigma(f_{\text{NL}})$	$\sigma(\Omega_{\text{DE}})$	$\sigma(w)$	$\sigma(f_{\text{NL}})$	$\sigma(\Omega_{\text{DE}})$	$\sigma(w)$	$\sigma(f_{\text{NL}})$
HSC1	0.030	0.151	240.4	0.012	0.189	37.8	0.010	0.103	8.1
HSC2	0.023	0.108	188.2	0.011	0.142	28.0	0.009	0.074	6.2
DES	0.032	0.081	210.6	0.011	0.102	35.3	0.009	0.055	7.9
LSST	0.009	0.037	106.1	0.006	0.051	6.9	0.005	0.024	1.9

TABLE I: Marginalized constraints on cosmological parameters estimated from the Fisher matrix analysis using the number counts and/or the variance of counts (clustering). WMAP5 cosmology is assumed as a fiducial model. Constraints in four future survey parameters, HSC1 (1000 deg², $z_{\text{max}} = 1.4$), HSC2 (2000 deg², $z_{\text{max}} = 1.4$), DES (5000 deg², $z_{\text{max}} = 1.0$), and LSST (20000 deg², $z_{\text{max}} = 1.7$), are presented.

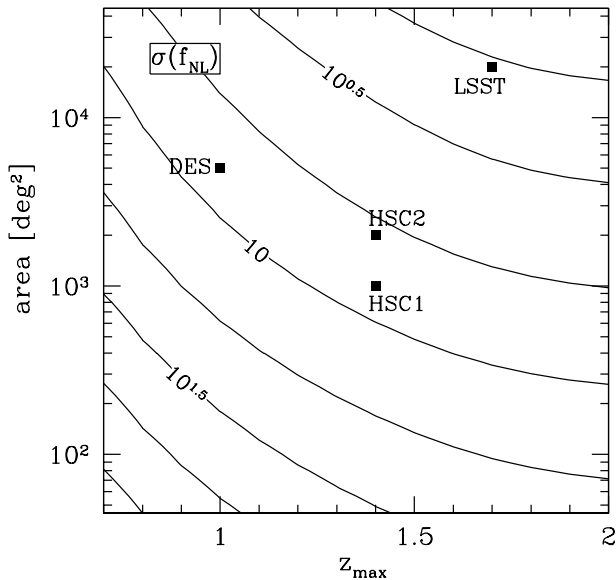


FIG. 3: Expected marginalized constraints on f_{NL} as a function of two survey parameters, the survey area and the maximum redshift z_{max} . Contours are drawn per 0.25 dex. Four survey parameters considered in this paper are indicated by filled squares.

affects our results [12, 13]. The impact of other systematics, such as cluster photometric redshifts [14] and the effect of halo assembly bias [25], should be addressed. On the other hand, we used only the count variance of each cell as the clustering information. Since the effect of primordial non-Gaussianity is more significant at larger scales, including the count covariance (or including the full clustering information with the power spectrum [11]) may improve the constraints further. We leave such more comprehensive treatments for future work.

This work was supported by Department of Energy contract DE-AC02-76SF00515.

* Electronic address: oguri@slac.stanford.edu

[1] N. Bartolo *et al.*, Phys. Rept. **402**, 103 (2004)

- [arXiv:astro-ph/0406398].
- [2] A. P. S. Yadav and B. D. Wandelt, Phys. Rev. Lett. **100**, 181301 (2008) [arXiv:0712.1148].
- [3] E. Jeong and G. F. Smoot, arXiv:0710.2371; E. Komatsu *et al.* [WMAP Collaboration], Astrophys. J. Suppl. **180**, 330 (2009) [arXiv:0803.0547]; C. Hikage *et al.*, Mon. Not. Roy. Astron. Soc. **389**, 1439 (2008) [arXiv:0802.3677]. A. Curto *et al.* arXiv:0807.0231.
- [4] N. Dalal *et al.*, Phys. Rev. D **77**, 123514 (2008) [arXiv:0710.4560].
- [5] S. Matarrese and L. Verde, Astrophys. J. **677**, L77 (2008) [arXiv:0801.4826].
- [6] A. Slosar *et al.*, JCAP **0808**, 031 (2008) [arXiv:0805.3580].
- [7] N. Afshordi and A. J. Tolley, Phys. Rev. D **78**, 123507 (2008) [arXiv:0806.1046].
- [8] V. Desjacques, U. Seljak and I. Iliev, arXiv:0811.2748
- [9] M. LoVerde *et al.*, JCAP **0804**, 014 (2008) [arXiv:0711.4126].
- [10] E. Sefusatti *et al.*, Astrophys. J. **658**, 669 (2007) [arXiv:astro-ph/0609124].
- [11] S. Majumdar and J. J. Mohr, Astrophys. J. **613**, 41 (2004) [arXiv:astro-ph/0305341].
- [12] M. Lima and W. Hu, Phys. Rev. D **70**, 043504 (2004) [arXiv:astro-ph/0401559].
- [13] M. Lima and W. Hu, Phys. Rev. D **72**, 043006 (2005) [arXiv:astro-ph/0503363].
- [14] M. Lima and W. Hu, Phys. Rev. D **76**, 123013 (2007) [arXiv:0709.2871].
- [15] D. J. Eisenstein and W. Hu, Astrophys. J. **496**, 605 (1998) [arXiv:astro-ph/9709112].
- [16] M. S. Warren *et al.*, Astrophys. J. **646**, 881 (2006) [arXiv:astro-ph/0506395].
- [17] N. Sugiyama, Astrophys. J. Suppl. **100**, 281 (1995) [arXiv:astro-ph/9412025].
- [18] R. K. Sheth and G. Tormen, Mon. Not. Roy. Astron. Soc. **308**, 119 (1999) [arXiv:astro-ph/9901122].
- [19] W. Hu and B. Jain, Phys. Rev. D **70**, 043009 (2004) [arXiv:astro-ph/0312395].
- [20] J. Dunkley *et al.* [WMAP Collaboration], Astrophys. J. Suppl. **180**, 306 (2009) [arXiv:0803.0586].
- [21] <https://www.darkenergysurvey.org/>
- [22] <http://www.lsst.org/lsst>
- [23] P. Serra and A. Cooray, Phys. Rev. D **77**, 107305 (2008) [arXiv:0801.3276].
- [24] C. Carbone, L. Verde and S. Matarrese, arXiv:0806.1950.
- [25] H. Y. Wu, E. Rozo and R. H. Wechsler, Astrophys. J. **688**, 729 (2008) [arXiv:0803.1491].